Journal of Marine Science and Engineering

MDPI

Article

Evaluating Mooring Line Test Procedures Through the Application of a Round Robin Test Approach

Faryal Khalid [1]*, Peter Davies [2], Peter Halswell [1], Nicolas Lacotte [2], Philipp R. Thies[1] and Lars Johanning [2,3]

[1] College of Engineering, Mathematics and Physical Sciences, University of Exeter, Treliever Road, Penryn, Cornwall TR10 9FE, UK; p.halswell@exeter.ac.uk (P.H.); p.r.thies@exeter.ac.uk (P.R.T.)
[2] IFREMER Centre Bretagne, Marine Structures Laboratory, 29280 Plouzané, France; peter.davies@ifremer.fr (P.D.); nicolas.lacotte@ifremer.fr (N.L.); l.johanning@exeter.ac.uk (L.J.)
[3] Naval Architecture and Ocean Engineering, Harbin Engineering University, Harbin 150001, China
* Correspondence: f.khalid2@exeter.ac.uk

Received: 30 April 2020; Accepted: 11 June 2020; Published: 13 June 2020

Abstract: Innovation in materials and test protocols, as well as physical and numerical investigations, is required to address the technical challenges arising due to the novel application of components from conventional industries to the marine renewable energy (MRE) industry. Synthetic fibre ropes, widely used for offshore station-keeping, have potential application in the MRE industry to reduce peak mooring line loads. This paper presents the results of a physical characterisation study of a novel hybrid polyester-polyolefin rope for MRE mooring applications through a round robin testing (RRT) approach at two test facilities. The RRT was performed using standard guidelines for offshore mooring lines and the results are verified through the numerical modelling of the rope tensile behaviour. The physical testing provides quantifiable margins for the strength and stiffness properties of the hybrid rope, increases confidence in the test protocols and assesses facility-specific influences on test outcomes. The results indicate that the adopted guidance is suitable for rope testing in mooring applications and there is good agreement between stiffness characterisation at both facilities. Additionally, the numerical model provides a satisfactory prediction of the rope tensile behaviour and it can be used for further parametric studies.

Keywords: synthetic fibre ropes; testing infrastructure; round robin testing; rope modelling; mooring components; marine renewable energy

1. Introduction

Emerging technologies, such as marine renewable energy (MRE), readily adopt components and standard guidance from conventional industries for a novel application. To de-risk industrial innovation in MRE, the experience from conventional industrial application must be combined with the knowledge of the application area. This can be done through an integrated approach involving comprehensive numerical modelling, and a dedicated component physical testing programme, as well as field demonstrations.

Synthetic fibre ropes were proposed for deep-water moorings of floating offshore oil and gas platforms by Del Vecchio nearly 30 years ago [1], and are now widely accepted [2,3]. The low linear density of polyester fibre ropes compared to steel wire and chain has made them the preferred choice beyond 1500 m depth. In addition, service experience since the 1990s has been very positive [4]. Fibre ropes could also offer significant advantages for MRE applications through peak load reduction [5], but a thorough technology assessment must be conducted to quantify risks and uncertainties.

Weller et al. [6] reviewed the possibilities for mooring floating offshore wind, wave and tidal energy installations. Although the mooring system designs are similar (i.e., catenary or taut-leg

geometries), large manned platforms for oil and gas production are designed with natural periods, which avoid the expected first order wave periods of the area. Excitation by longer period, second order wave forces may be allowed if levels of component fatigue cycling are acceptable. In contrast, wave energy recovery devices are designed so that the natural periods of one or more modes of motion correlate with the expected wave energy periods, in order to maximise the level of energy absorbed for a given location. This can result in highly dynamic device responses, which are directly coupled to the response of the mooring system. The requirements for floating offshore wind are closer to those of the oil and gas industry, but the platforms are smaller and are subjected to larger movements. In this case, more mooring line compliance is needed to avoid generating high cyclic loads and materials such as polyester may be too stiff; therefore, there has been considerable recent interest in polyamide ropes for this application [7–9].

Ropes are based on repeating elements, but their hierarchical construction and the large number of material possibilities make them complex engineering structures.

First, there is a wide range of polymer fibres available and families of fibres, such as the polyesters or nylons, include many grades [10]. The drawing conditions and ratios of these fibres can be tailored to some extent to produce a range of properties, and the widespread use of proprietary coatings limits the possibility of defining generic datasheets.

A second level of complexity comes from the rope construction itself. Rope may be braided or twisted, and rope-making machines can manufacture a range of products by changing twisting and braiding parameters, at levels from single yarns up to strands [10]. Differences in ropemaking equipment and practice are reflected in variable stiffness properties, as was noted in early work on polyester ropes for offshore mooring lines [11].

A further degree of complexity can be added by combining different fibres within the same rope. This is an area that has received little attention, but many ropemakers provide products involving two fibres. The most common example is the combination of load-bearing cores of one fibre with a braided outer cover of a second fibre. Two fibres can also be used within the core, as is the case for the specimen studied in the present paper (polyester and polyolefin fibres). This requires careful consideration of the mechanical response of each fibre in order to get the best estimate of combined performance. An example in the high-performance fibres market is the BOB™ product [12], which combines HMPE fibres with liquid crystal polyester fibres, in order to improve the high temperature performance of HMPE for bend over sheave applications. A more radical development to reduce peak loads is the combination of an outer fibre rope construction with an inner elastomeric core, known as the Exeter Tether [13]. In this case, two separate functions are combined, allowing the tether to respond in different ways to small and large displacements.

To increase confidence in the application of synthetic fibre rope mooring components in the MRE industry, their tensile stiffness and strength properties must be investigated. While field-testing provides the opportunity to understand in situ rope behaviour, it is associated with high risk and test cost. Purpose-built test facilities [14], operated by rope manufacturers or research and academic institutes, provide a relatively inexpensive alternative for synthetic rope characterisation. Although these facilities provide a similar range of services, large variation exists in the test set-up and available instrumentation that may influence the implementation of test procedures and rope characterisation. Independent calibrations and certifications are regularly conducted at most facilities, but no comparative study has been conducted yet, regarding the influence of test infrastructure on the performance characterisation. To this end, a round robin testing (RRT) approach may be employed to assess the variability in outcomes due to test implementation. An RRT approach is an experimental methodology that informs the reproducibility of a test practice through independent testing and analysis at multiple laboratories [15]. The RRT method has been readily adopted in the environmental [16], manufacturing [15], materials [17] and renewable energy [18] industries. Conducting an inter-facility mooring RRT provides the opportunity to correlate and quantify the influence of individual test facilities on the mooring characterisation, by repeated implementation of the same test program adopted from standard guidance on multiple samples.

The aims of this paper are twofold: first, to characterise the strength and stiffness of a hybrid fibre rope as a candidate for MRE mooring applications. Second, to critically evaluate the test procedures available for this type of application, by discussing results from tests performed on ropes from the same batch in two test laboratories in the UK and France, using the same ISO test procedure developed for offshore moorings [19].

2. Materials and Methods

This section describes the test specimen—a hawser laid rope with hybrid yarns consisting of polyester fibres wound round polyolefin—and the physical and numerical test methods. It provides details of the involved test infrastructure, presents the test protocol and introduces the rope modelling software.

2.1. Test Specimen

The material selected for this study is a hybrid polyester-polyolefin fibre yarn in a twisted rope construction, as shown in Figure 1. This rope is currently produced for mooring tails, showing higher strength than nylon at a given diameter, lower sensitivity to water and lower linear density than polyester (PET). Table 1 summarises rope specifications provided by the manufacturer including minimum breaking load (MBL) and Table 2 presents an overview of the rope construction.

Table 1. Rope parameters provided by the manufacturer.

Rope reference	EUROFLEX™ 3-strand
Diameter	32 mm
Linear density	59.5 kg/100 m
Minimum Break Load (MBL)	168 kN

Table 2. Rope construction displaying the elements and material properties of the test sample.

Level	Elements
Rope	3 strands
Strand	23 rope yarns
Rope yarn	2 hybrid yarns
Hybrid yarn	Polyester and Polyolefin

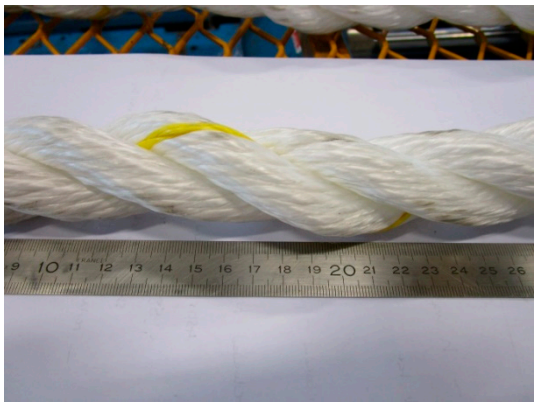

Figure 1. Twisted rope construction of the hybrid polyester-polyolefin rope.

Five rope samples were tested at each facility. The overall length of each sample was 5 m and spliced eye terminations allowed 2.5 m of unspliced rope for testing. Samples at DMaC were respliced and further reduced in length to allow for the additional elasticity of the rope, in order to conduct successful load-to-failure tests.

2.2. Rope Yarn Tests

First, tensile tests were performed on rope yarns in order to examine the behaviour of one of the basic rope elements. These consisted of two hybrid yarns twisted together, as displayed in Figure 2. The yarns were gripped in special pneumatic grips and pulled to failure on an Instron™ 5966 tensile test machine (Figure 3), at a loading rate of 50 mm/min.

A 10 kN load cell was used to record the force. The strain was measured by both the crosshead movement and a camera extensometer system. New samples were not available, so rope yarns were extracted from a rope sample that had been tested to failure, taking samples from the spliced loop at the opposite end to the failed region. No visual damage was apparent in this area, but given the previous loading cycles to measure stiffness (see Section 2.4 below), these samples can be considered to be well bedded-in.

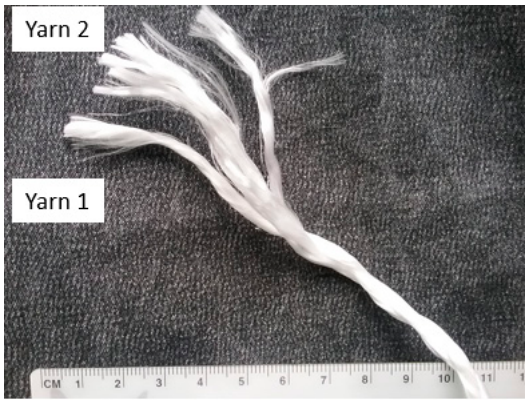

Figure 2. Image of double hybrid yarn with intact Yarn 1 (left) and disassembled Yarn 2 (right).

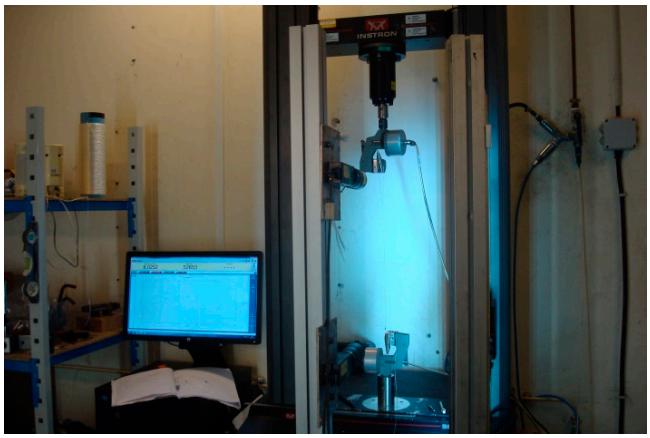

Figure 3. Hybrid yarn tensile test set-up.

2.3. RRT Facilities

Two test facilities, namely the Dynamic Marine Component (DMaC) test facility at the University of Exeter and The Marine Structures laboratory at L'Institut Français de Recherche pour l'Exploitation de la Mer (IFREMER), were involved in the RRT of the hybrid rope. Figure 4 shows the test set-up at the two facilities where the RRT was conducted.

While both facilities provide similar test capabilities, the instrumentation involved in test set-up, test implementation, maintaining ambient conditions and data logging is considerably different. Table 3 compares the instrumentation at the facilities relevant to this study.

(a) (b)

Figure 4. Test set-up at (**a**) Dynamic Marine Component (DMaC) and (**b**) L'Institut Français de Recherche pour l'Exploitation de la Mer (IFREMER).

Table 3. Instrumentation at DMaC and IFREMER for Round Robin Testing (RRT) campaign.

Instrumentation	Parameter	DMaC	IFREMER
Load cell	Type	Applied Measurement Ltd. DSCC pancake	AEP TC4
	Maximum dynamic force	20 tonnes	30 tonnes
Transducer	Quantity	1	2
	Type	WS12-1000mm draw-wire	ASM WS10-500mm & WS10-1250mm draw-wires
	Mounting	Clamped on rope	L frame
Piston displacement	Measurement	RLS Merilna tehnika d.o.o., Slovenia LM10 linear encoder	SCAIME wire transducer model PT5DC-40
Data logger	Type	National Instruments compact Reprogrammable Input Output (cRIO) 9022	MTS MultiPurpose Elite software
Other	Wetting process	Submerged samples	Continuous spray

Both facilities used a pancake load cell with different load ratings and similar accuracy (linearity—DMaC 0.039%, IFREMER 0.05%) to measure tensile load. DMaC performs in-house calibration on their load cell, using a reference load cell that is calibrated by an external company and traceable to National Physical Laboratories. IFREMER calibrates their load cell using an accredited external company. Both facilities perform annual calibrations.

Draw-wire transducers were used at both facilities with similar accuracy (linearity—DMaC 0.05%, IFREMER 0.1%) to measure the gauge length. At DMaC, the transducer body was clamped to the rope sample using a custom-made clamp and the wire length was extended via an additional length of wire, to ensure the gauge length was greater than 1.2 m. The wire-end was attached to the sample using a bungee cord. At IFREMER, the draw-wire transducers were mounted on an L frame at the two ends of the sample, to ensure that they were at an appropriate height to measure elongation. The wire ends were attached to the central section of the rope with bungee cords to measure elongation.

DMaC uses a magnetic linear encoder and IFREMER uses a draw-wire sensor to measure piston displacement. The piston displacement was used to measure elongation during the load-to-failure tests, as the draw-wire transducers risk damage during the break tests.

Both test facilities use synchronised control and data logging systems to control piston displacement and record measurements. For this RRT campaign, data acquisition frequency of 50 Hz was used at DMaC, whereas, at IFREMER, it was 1 and 10 Hz.

To reflect the intended application of the ropes, samples were continuously wetted throughout testing. Different sample wetting methods were used at each facility. At DMaC, the samples were fully submerged in fresh water during testing, whereas, at IFREMER, samples were sprayed with fresh water throughout the test protocol, except during the load-to-failure tests.

2.4. RRT Test Protocol

A standard test procedure, based on the ISO 18692:2007(E) guidance [19] for pure polyester ropes, was implemented as shown in Figure 5. This test protocol can be divided into Phase A and Phase B as shown in Figure 5 and Table 4. Each phase provides significant information for rope characterisation: Phase A informs the rope stiffness and Phase B quantifies the rope strength.

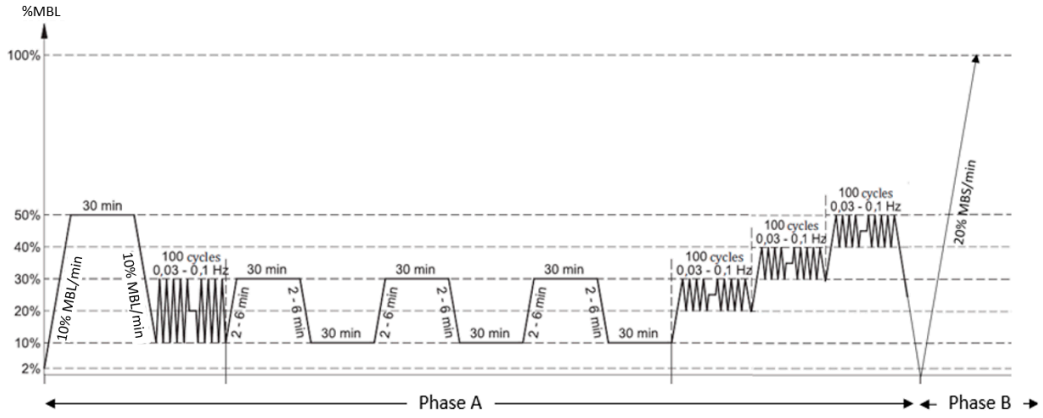

Figure 5. Schematic of test sequence (adapted from ISO standards [20]).

Table 4. Description of constituent steps of ISO18692:2007 in Phase A and Phase B.

Phase	Characterisation	Steps	Description
Phase A	Stiffness	6, 7	Bedding-in (static)
		8	Bedding-in (dynamic)
		9	Quasi-static loading Dynamic loading
Phase B	Strength	10	Load-to-failure

Since the adopted standard provides guidance for testing pure polyester fibre ropes used for offshore station-keeping of permanent or mobile floating structures, three different test regimes were employed to ascertain the suitability of the standard to the polyester-polyolefin blend. These regimes and the associated test durations are summarised in Table 5.

Table 5. Description and duration of the test regimes employed for RRT of a fibre rope.

Test Regime	Description	Test No.	Test description	Duration
1	Repeatability	Test 01 Test 02 Test 03	Phase A → Phase B	5 h 50 min 20 s
2	Rest period variation	Test 04	Phase A → Rest → Phase B	23 h 50 min 20 s
3	Cycling variation	Test 05	Phase A → Rest → Phase A → Phase B	34 h 50 min 20 s

Test Regime 1, the implementation of the standard protocol [19], was repeated three times at each facility, to provide a quantifiable margin for the break strength relative to the MBL specified by the manufacturer. Test Regime 2 was designed to investigate the influence of varying the rest period between Phase A and Phase B on the achieved break strength. Furthermore, Test Regime 3 was designed to study the possible effect of dynamic loading on the achieved MBL. Only one sample was tested under Test Regimes 2 and 3 at each facility.

For the overnight rest periods in Test Regimes 2 and 3, the samples were detached at one end to remove the load completely, but were left submerged at DMaC and sprayed at IFREMER throughout the rest period.

2.4.1. Sample Preparation

The effective performance characterisation of synthetic ropes for offshore station-keeping applications necessitates that the samples are soaked in water prior to testing. For this study, all the samples were soaked in fresh water overnight to account for the influence of water ingress on the rope stiffness and strength parameters. After installing the sample and the wire transducer(s), a load equivalent to 2% MBL (3 kN) was applied to the sample to measure a reference length, L_R. At DMaC, L_R is the gauge length at reference tension, whereas, at IFREMER, it is the distance between the attachment points of the two transducers.

As identified in Table 4, the samples are bedded-in at the start of the test. Bedding-in allows the redistribution of loads betwen different elements of the rope assembly. Permanent elongation is caused at microscopic level by the alignment of molecules in the direction of stress, resulting in non-recoverable, residual strain. At macroscopic level, it is caused by the rope elements settling into the most efficient load path, due to the local adjustment of the constituent fibres, yarns and strands. The fibre rope and end terminations display elongation under steady and cyclic loading, therefore, it is standard practice to apply a combination of both to bed-in the rope assembly. Bedding-in can significantly increase rope stiffness and reduce the damping capacity, therefore, it must be considered in design [5].

For the RRT, the rope was bedded-in by applying a static and dynamic load. For the static bedding-in, a load equivalent to 50% of the MBL was applied at a rate of 10% MBL/min. This load was maintained for 30 min and then the rope was unloaded to 10% MBL at the same load rate. This was followed by 100 cycles of dynamic bedding-in between 10% and 30% MBL with 15 s period.

2.4.2. Stiffness Characterisation

The performance of the polyester-polyolefin blend is characterised by stiffness values calculated at the end of bedding-in and for quasi-static and dynamic loading, based on the implementation of Phase A of the test plan. Two elongation measurements are recorded for Phase A of each test, namely, piston displacement and changes in gauge length. However, since the piston displacement includes the displacement of eye splices and end loops, it does not provide accurate stiffness values. Therefore,

gauge measurements are used for determining stiffness parameters of the samples for steps in Phase A.

The conventional representation of tensile behaviour of materials is a stress-strain plot, however, for rope structures, this requires a cross-section to be defined. This introduces a source of error, as ropes are not fully compacted, therefore, force-strain plots are presented as stiffness indicators in this paper, to enable results to be compared directly without including an additional uncertainty. As the rope linear density is easier to measure, this is often used, and a specific stress can then be defined as the ratio of force and linear density.

The resulting stiffness for the tests is calculated by the relationship between the change in applied load and resulting elongation (measured by changes in gauge length), based on Equation (1).

$$K = \frac{\Delta F}{\frac{e}{L_R} \times 100} \quad (1)$$

where K (kN/%) is the stiffness indicator, F (kN) is the force and e (m) is the gauge length elongation, respectively.

As discussed earlier, the method to determine elongation measurements varies between DMaC (one transducer) and IFREMER (two transducers), due to the different instrumentation. The elongation at both facilities can be calculated by Equation (2):

$$e = L_G - L_R \quad (2)$$

where L_G (m) is the final gauge length.

The stiffness at the end of bedding-in is calculated as the slope of a linear regression of the force-strain data points measured during the last five cycles in the 10-30% MBL load range.

Quasi-static stiffness is quantified as the secant stiffness between the end points of successive half-cycles [19]. Three representative quasi-static load cycles were applied between 10-30% MBL at the load rate of 5% MBL/min, and a hold of 30 min was prescribed at each step. Quasi-static stiffness is calculated as:

$$K = \frac{F_{30} - F_{10}}{\frac{e_{30} - e_{10}}{L_R} \times 100} \quad (3)$$

where, F_{30} and e_{30} are the load and elongation at 30% MBL, respectively. Similarly, F_{10} and e_{10} are the load and elongation at 10% MBL.

The stiffness of the first quasi-static cycle is excluded from the calculation. This is because the rope does not reach equilibrium before quasi-static reloading starts after dynamic bedding-in.

Dynamic stiffness is representative of the near-linear behaviour of synthetic ropes observed under cycling due to wave action [19]. To quantify the dynamic stiffness of the rope, three load ranges are specified in the order of 10% of the MBL. For the RRT, the chosen load ranges are 20-30% MBL, 30-40% MBL and 40-50% MBL, respectively. At each load range, 100 cycles are applied. The dynamic stiffness for each load range is defined as the slope of all the force-strain pairs recorded during the last five loading cycles for the respective load range.

2.4.3. Strength Characterisation

Load-to-failure tests, as per Phase B of the test plan, allow for the verification of the tensile break load of the rope against the MBL specified by the manufacturer. This involves loading the sample at a rate of 20% MBL/min until it fails.

2.5. Rope modelling

In order to examine some rope construction parameters, simulations were performed using the Fibre Rope Modeller (FRM) software from Tension Technology International (TTI).

The FRM software models the rope structure in a hierarchical fashion, much the same as the rope making process. A basic element, such as the fibre yarn, is specified at the outset of the modelling

process. This element is characterised by its density, diameter, load-extension behaviour and break strength. The model then allows for a description of the assembly of the element into the next hierarchical level through specification of the number of elements, their associated spatial position and degree of twist. This is repeated at all hierarchical levels. It is then necessary to relate the tensions, elongations, torques and twists applied to the entire rope structure to those imposed on the individual rope elements. This is done using the principle of virtual work [21] which dictates that the combined work performed by a given tension to change the rope length and the work performed by a torque to change the rope twist are equal to the overall work performed on all elements of that rope. Changes in length and twist are applied to the highest-level structural element, the rope. The rope structural model calculates the resulting changes in length and twist on the subsequent lower level, down to the smallest elements.

In a perfect rope structure, all elements share the load equally and they all reach the failure strain at the same time. In real ropes, load sharing is not uniform, due to multiple factors. This includes unequal tensions during the rope making process, different lengths along the helical paths, non-linear stress-strain characteristics of synthetic material fibres, statistical variations and the compaction of elements.

The model programme can account for all of the important aspects mentioned above. Thus, it is able to predict which element will reach breaking strain and undergo failure first, along with the imposed elemental conditions of the failure. It can then calculate the loss of the load-carrying ability of that element and will transfer that load to neighbouring elements. The changes in strain in those adjacent elements and the resulting change in overall rope length are also determined. Failure of one or several elements may cause the adjacent elements to fail immediately, resulting in either complete failure or strength loss. Further details can be found in [22–25].

3. Results

The results of the rope yarn testing, RRT and rope modelling are presented in this section.

3.1. Rope Yarn Tests

Figure 6 shows an example of the stress-strain response of a single hybrid yarn. Stress is calculated as force normalised by linear density in tex (g/km).

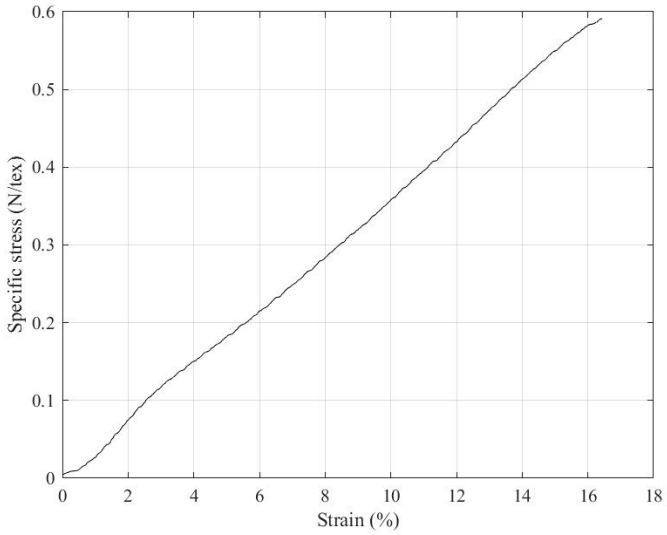

Figure 6. Stress-strain relationship for the polyester-polyolefin hybrid yarn.

As observed, the response is quite linear, with a small knee on the curve around 2% strain, typical of the behaviour of PET filaments [26].

3.2. RRT at DMaC and IFREMER

A comparison between RRT results at DMaC and IFREMER is presented for the following parameters:

- End of bedding-in stiffness;
- Quasi-static stiffness;
- Dynamic stiffness;
- Failure behaviour.

The results are presented as percent deviation, D_k, of the sample stiffness, K_s, from the mean stiffness, K_m, using the formulation in Equation (4).

$$D_k = \frac{K_s - K_m}{K_m} \times 100 \quad (4)$$

For Test 05 at each facility, two stiffness values are shown. Test 05a represents the first implementation of Phase A and Test 05b presents the stiffness values for the second implementation of Phase A after being left unloaded overnight.

3.2.1. First Loading and Bedding-in

The responses of the five samples during first loading (up to 50% MBL) at DMaC and IFREMER are shown in Figure 7.

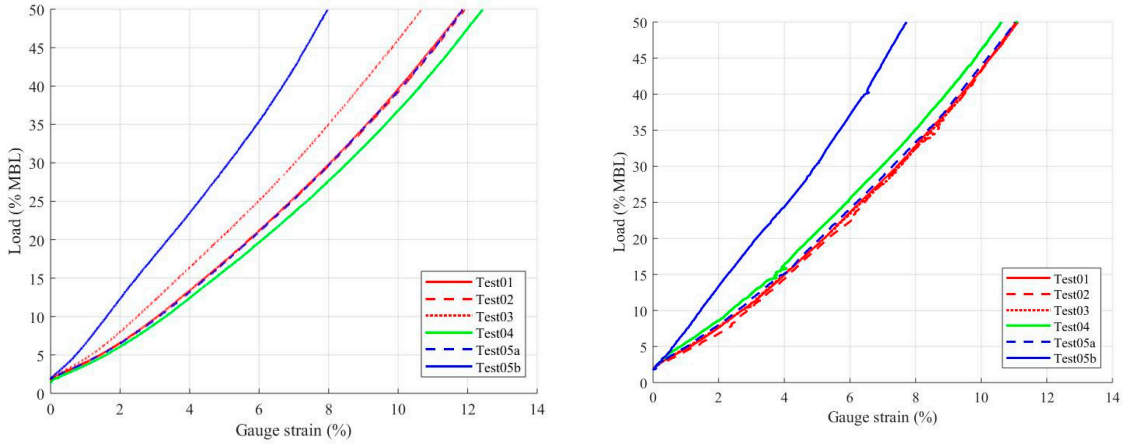

Figure 7. First loading of samples at (a) DMaC and (b) IFREMER.

It can be observed that the initial load-strain behaviour of the samples is similar at both facilities, with a maximum strain at 50% MBL of around 11%. A higher stiffness is observed at both facilities for Test 05b, since the rope has already been subjected to the sequence of loads up to 50%MBL once, during Test 05a.

K_d of the various test specimens after the dynamic bedding-in is presented in Figure 8a for a K_m value of 28.9 kN/%, calculated from Test 01 to Test 05a (Test 05b is excluded) at both facilities. In this case, stiffness at both facilities shows less than 12.5% deviation from the mean, including the measurement in Test 05b. The variance of the measurements at IFREMER is lower than at DMaC.

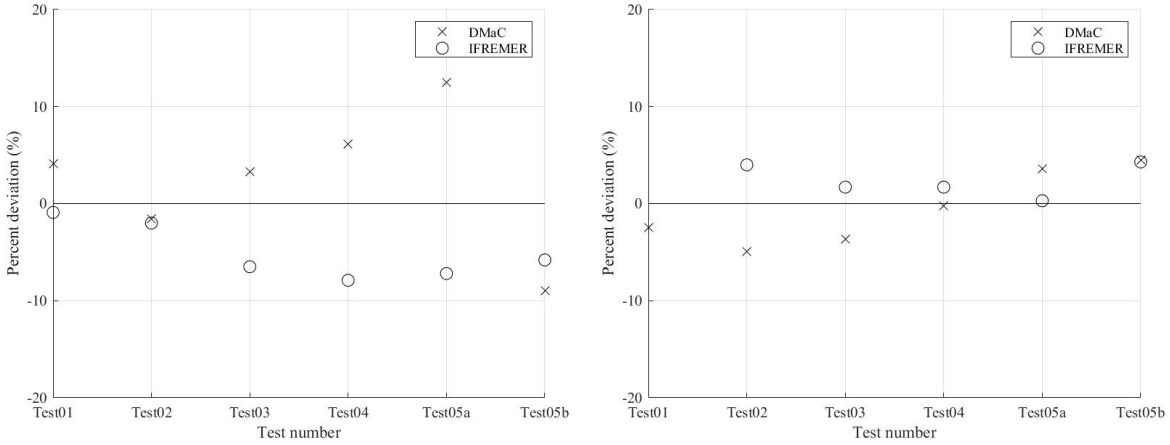

Figure 8. RRT percent deviation of (**a**) End of bedding-in stiffness from mean value of 28.9 kN/% and (**b**) Quasi-static stiffness from the mean stiffness value of 17.4 kN/%.

The elongation time series for all samples show that the rope exhibited negligible elongation gain after the implementation of 75 dynamic bedding-in cycles, therefore, was fully bedded-in by implementing the test protocol.

3.2.2. Quasi-Static Stiffness

The average percent deviation of the quasi-static stiffness within the various test specimens for the last two quasi-static cycles is shown in Figure 8b. The K_m value for the quasi-static stiffness, 17.4 kN/%, is calculated from Test 01 to Test 05a for DMaC and Test 02 to Test 05a for IFREMER. Test 05b is excluded for both facilities, whereas quasi-static stiffness results from Test 01 at IFREMER are not available due to testing problems.

The quasi-static stiffness values at both facilities show good agreement, with a percent deviation of less than 5% from the mean stiffness value. Once again, the variance in quasi-static stiffness is lower at IFREMER relative to DMaC samples

3.2.3. Dynamic Stiffness

The percentage deviation of dynamic stiffness values for the three specified dynamic load ranges (20–30% MBL, 30–40% MBL and 40–50% MBL) can be seen in Figure 9. The mean values for the dynamic stiffness are 31.4 kN/%, 34.5 kN/% and 37.5 kN/% for each load range, respectively. These K_m values are calculated from Test 01 to Test 05a, for both DMaC and IFREMER (Test 05b is not included).

For the dynamic stiffness characterisation, the deviation at IFREMER is within 15% of the mean, relative to 10% for DMaC at all applied cyclic load ranges. In contrast to the quasi-static stiffness, variance in the dynamic stiffness measurements at DMaC is observed to be lower than at IFREMER.

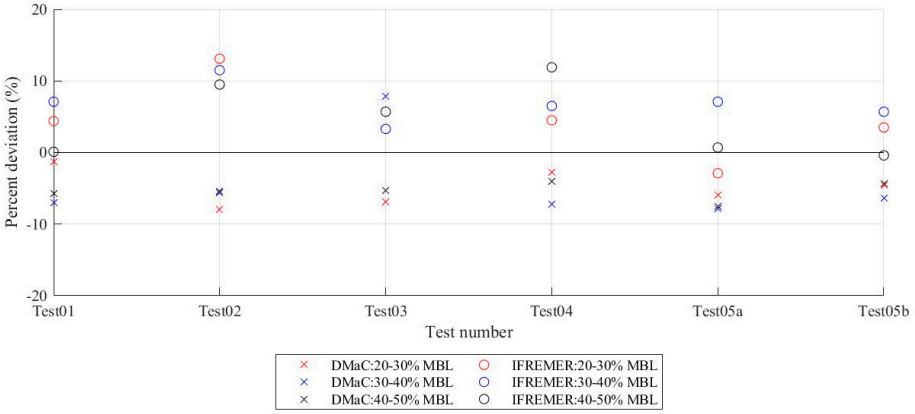

Figure 9. Percent deviation of dynamic stiffness at load ranges of 20–30% MBL, 30–40% MBL and 40–50% MBL, from mean stiffness values of 31.4 kN/%, 34.5 kN/% and 37.5 kN/%, respectively.

3.2.4. Load-to-Failure

The break loads of the various test specimens at each test facility are shown in Figure 10. The K_m value for the break load, 204 kN (121 % MBL), is calculated from Test 01 to Test 03 for DMaC and IFREMER. The break loads for Test 04 do not provide an accurate RRT comparison between facilities, since the sample at DMaC was too elastic to break after the rest period, despite three attempts. Test-to-failure was conducted after a further 24 h on a dry sample.

It can be seen that all samples at both facilities exceeded the break load specified by the manufacturer, some by up to 35%. Variance for break test measurements is lower at IFREMER than that at DMaC, as seen in Figure 10.

A failure mode investigation reveals that one strand failed for all ropes at or near the end of the eye splice at DMaC (Figure 11). Similarly, for IFREMER, the failure was due to one strand breaking at or near the splice, except Test 02, where all three strands broke in the eye splice. Rope failure at or near the splice is a commonly observed phenomenon, since the stress concentration at the splice introduces a weakness in the structural integrity of the rope assembly, causing a complete failure of the rope [27]. Ideally, the rope assembly would be at baseline strength if the eye splices are long and tapered, however, in practice, this is difficult to implement [28,29].

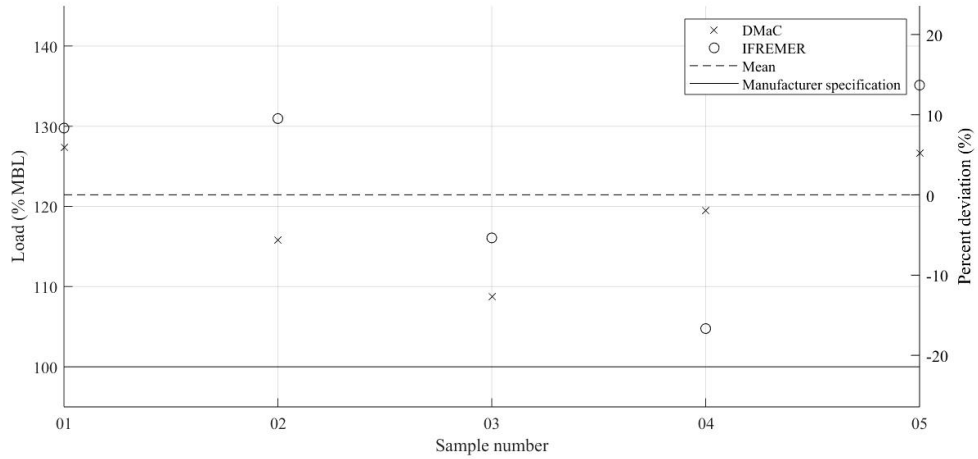

Figure 10. Load-to-failure RRT showing recorded break load and percent deviation from mean break load of 204 kN.

Figure 11. One broken strand near end of eye splice (Test 02 at DMaC), representative of the dominant failure mode.

4. Discussion

4.1. Confidence in Stiffness Measurements

RRT was conducted to investigate the confidence in rope characterisation at DMaC and IFREMER. Figure 12 shows the comparison between mean stiffness properties, determined at both facilities for various stages in the implemented test protocol. Figure 13 shows the comparison of the standard deviation in stiffness properties for the hybrid rope between the two facilities.

Based on the similarity of implementing Phase A on all five samples, statistical parameters for Phase A (dynamic bedding-in, quasi-static loading and dynamic loading) are calculated based on measurements from all five samples. It must be noted that the measurements from the second implementation of Phase A (Test 05b) and the quasi-static bedding-in of the specimen in Test 01 from IFREMER are excluded. As the implementation of Phase B was similar for Test 01, Test 02 and Test 03, these are used to calculate the mean break load of the samples at each facility.

Figure 12 shows that the mean stiffness values at IFREMER are higher than at DMaC, except for the stiffness value at the end of dynamic bedding-in. Figure 13 shows that the lowest deviation is observed for the quasi-stiffness, whereas the highest variability is for the break test at both facilities. In addition, the standard deviation between samples is higher at DMaC for all stages, except the three dynamic loading ranges. The inter-facility comparison in Figure 13 displays that the dynamic stiffness results are more precise at DMaC, whereas, the stiffness at the end of bedding-in, quasi-static and break stiffness are more precise for the tests performed at IFREMER. For both facilities, the quasi-static stiffness tests provide the most precise results, whereas the break tests have the lowest repeatability.

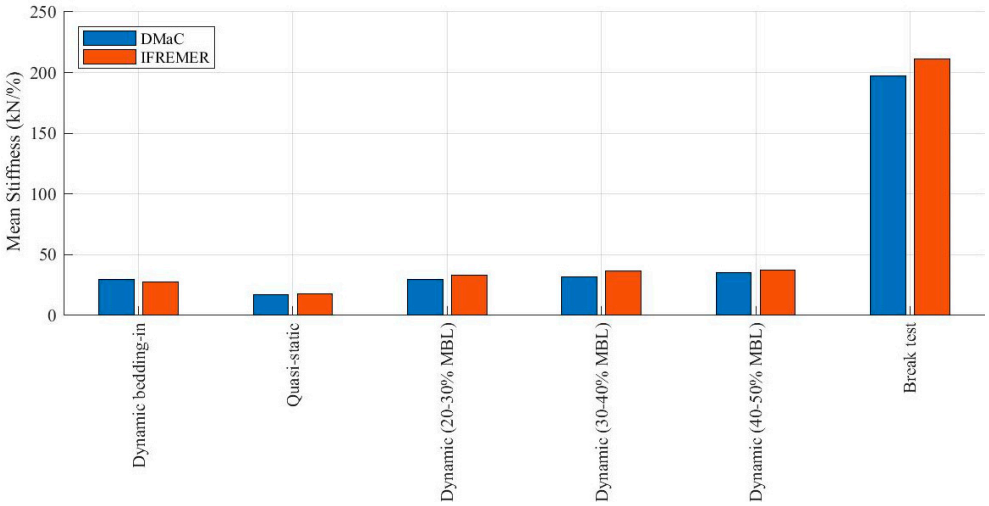

Figure 12. Comparison of the mean stiffness properties of the hybrid rope determined at DMaC and IFREMER.

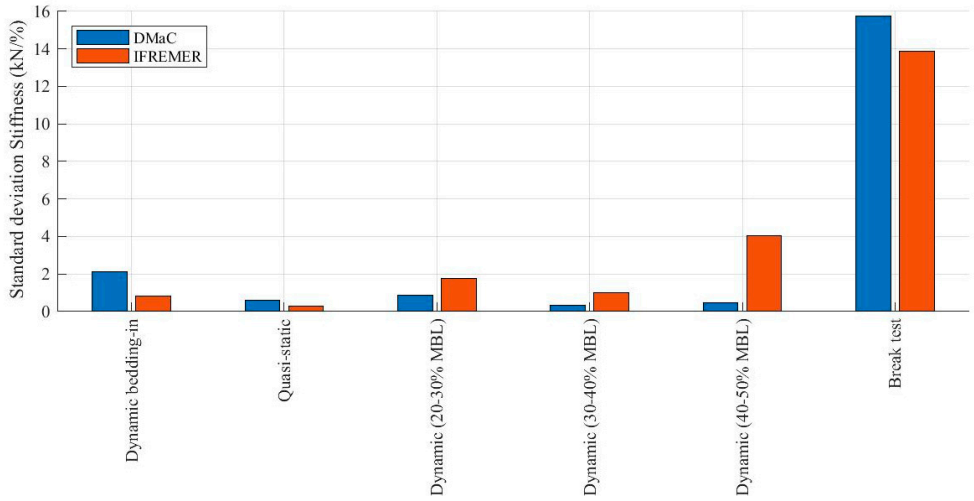

Figure 13. Comparison of the standard deviation in stiffness properties of the hybrid rope determined at DMaC and IFREMER.

The overall results can be regarded as accurate, since stiffness measurements between both facilities displays good agreement with a mean percentage difference of 8%, as seen in Figure 14. The quasi-static stiffness assessment provides the most accurate performance characterisation, with the least difference between both facilities. The dynamic stiffness values (for the mean range of 30–40% MBL) can be regarded as least accurate, since they display the largest difference between the facilities of over 10%.

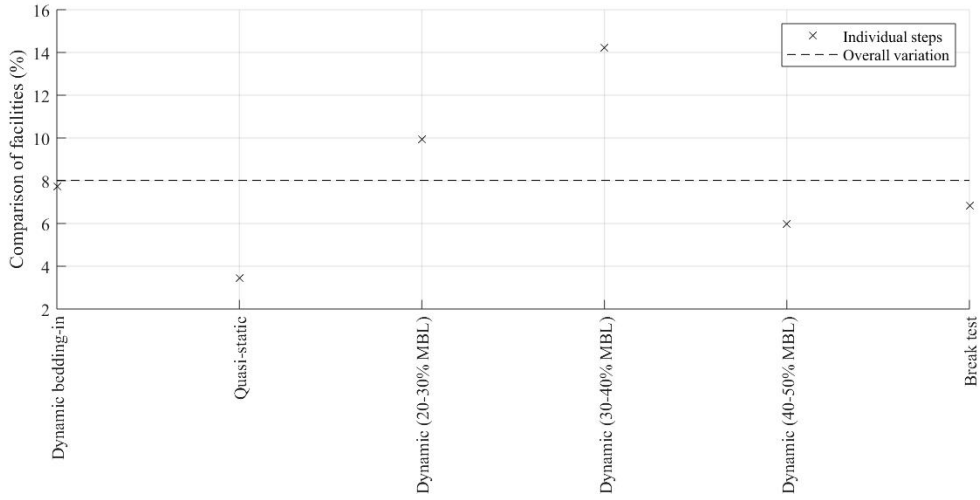

Figure 14. Percentage difference in mean stiffness values at both facilities, DMaC and IFREMER.

The differences in the statistical stiffness parameters can be attributed to sample or infrastructure variations. Change in length and sample resplicing at DMaC, albeit done with the same number of splice tucks, may have affected load transfer. The use of different load and strain transducers at the facilities and the varying data acquisition frequencies could also have been contributing factors. High sampling frequency allows for the improved capture of load peaks and may lead to a larger variation in test results.

4.2. Limits to Test Procedures

The guidance for pure polyester offshore mooring ropes based on ISO 18692:2007(E) [19] was found to be suitable for characterising the polyester-polyolefin blend. The applied test sequence included an initial bedding-in sequence and subsequent quasi-static and dynamic loading followed

by load-to-failure. The recommended bedding-in methodology for pure polyester was found to be sufficient for the relatively more elastic polyolefin blend.

However, the recommended cycling period of the dynamic bedding-in and stiffness characterisation is prescribed to be between 10 s and 33 s. This is not fully representative of the load conditions faced by some MRE devices, which may be subjected to additional higher frequency loads. A further analysis should be conducted at lower cycling periods of 3–5 s, to account for these effects on synthetic fibre rope performance.

Employing divergent test regimes did not significantly influence the break load results. This is in agreement with the standard guidance [19], which states that, after the initial bedding-in, further load-elongation cycles will not affect the break load of the rope. However, since only one test was conducted for Test Regimes 2 and 3 at each facility, further tests should be conducted to ensure the reproducibility of these results.

4.3. Comparison with Other Fibre Rope Options

It is interesting to compare the results from these tests with other candidate materials for MRE applications. Nylon and polyester are two such materials. Table 6 compares the dynamic stiffness, failure strain and density of these materials to the tested polyester-polyolefin blend. The stiffness values in Table 6 are expressed in a normalised form by dividing the stiffness indicators (Equation (1)) by the MBL and converting to strain rather than percentage strain.

Table 6. Comparison of the hybrid polyester-polyolefin sample with properties of other fibre ropes.

Rope product	Dynamic Stiffness 30-40% MBL	Failure strain, %	Density g/cm³	Source
Hybrid PET-Polyolefin	19-22	15-20	1.17	Present work
Nylon (PA6)	10	20-30	1.14	IFREMER data
Polyester (PET)	30	10-15	1.38	François [11]

The dynamic stiffness response of the hybrid rope is observed to be intermediate between 100% polyester and 100% nylon 6 ropes.

4.4. Comparison of Numerical Model Results and Physical Testing

The construction of the rope was modelled using the double rope yarn force-strain plot (Figure 6) as the input level. The resulting predicted rope force-strain behaviour, up to failure, is shown in Figure 15.

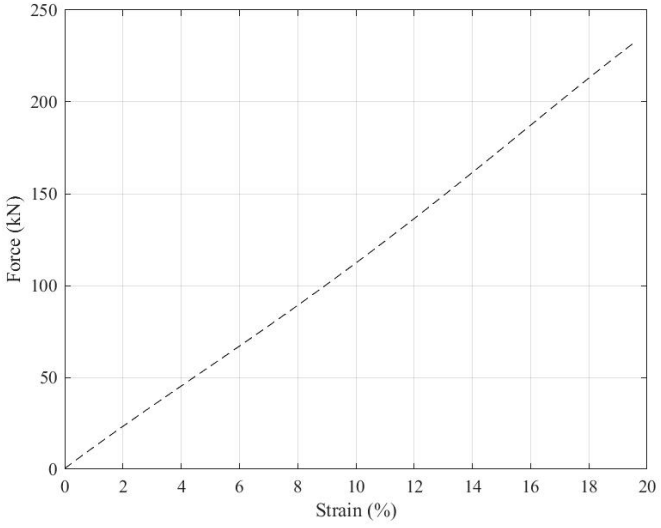

Figure 15. Modelled tensile force-strain behaviour of hybrid rope up to failure.

The predicted break load is significantly higher than the MBL specified by the manufacturer (168 kN). However, the achieved break load from load-to-failure tests are also higher for all samples at both facilities, as presented in Table 7.

Table 7. Predicted, measured and nominal break loads, kN.

FRM prediction	Measured values	Nominal MBL
233	218, 220, 195, 227, 176 214, 194, 183, 201, 213	168

The strain to failure was not measured in the central portion of the ropes in this study. This would require non-contact extensometry, to avoid introducing local stress concentrations (with clamps, for example) and prevent damage to the measurement device at failure. This means that only the break loads can be compared between the physical tests and numerical model, as shown in Table 7. It is interesting to compare the rope and yarn break stresses. This can be done by comparing the yarn failure stress (0.6 N/tex) with the range of break stresses for the ropes (0.3 to 0.38 N/tex), indicating a yarn efficiency in the range from 50 to 65%.

To compare an initial load force-strain plot with the rope model, only Test 05b can be used, as this is the only instance where the rope has already been bedded-in. Figure 16 shows this comparison at both facilities, as well as the initial loading plot for the first implementation of Phase A on the sample (Test 05a) at IFREMER.

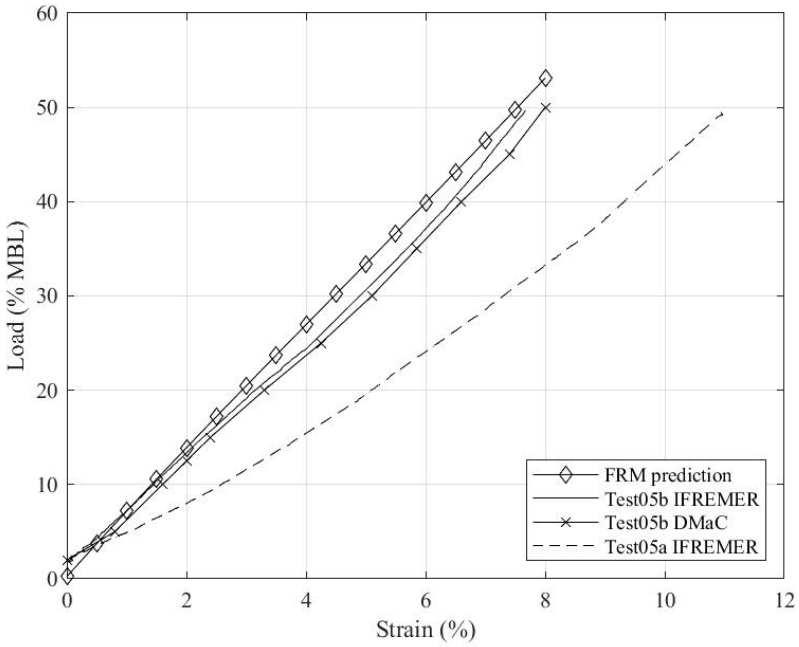

Figure 16. Comparison between modelled prediction of hybrid rope tensile force-strain behaviour and measured values up to 50% MBL for Test 05.

The usefulness of this rope model lies in the possibility to perform virtual studies of the influence of fibre type and rope construction parameters. To illustrate this, Figure 17 presents the influence of the lay length of the three twisted strands on the strain to failure for the hybrid rope.

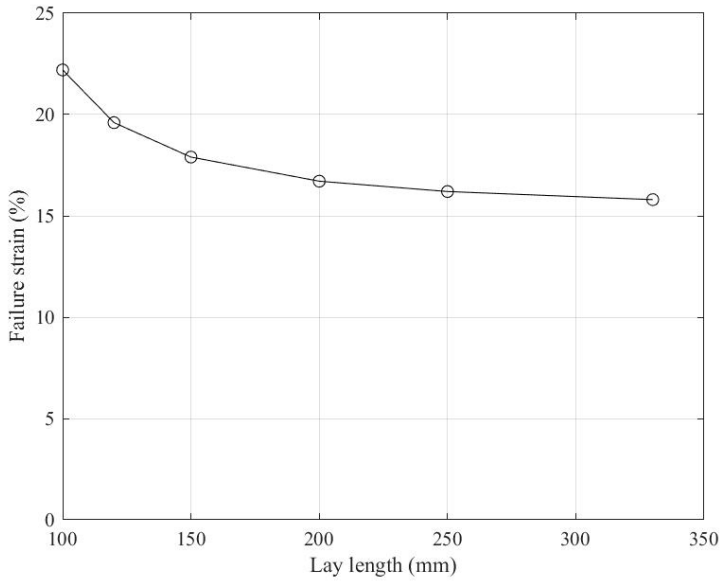

Figure 17. Influence of lay length on hybrid rope strain to failure.

Strain to failure increases as lay length is reduced, since the contribution to overall strain from geometrical effects increases. For a long lay length, the main elongation is due to the response of the fibre material itself. The influence on break load is smaller; over this range of lay lengths from 100 to 330 mm, the predicted load at failure increases from 227 to 250 kN. This suggests that increased energy absorption could be achieved in these ropes, by modifying construction parameters.

5. Conclusions

This paper provides a unique set of results from RRT on a hybrid rope for MRE mooring applications. These results indicate that tests performed independently in two test facilities give similar results, provided that a strict protocol is followed. An inter-facility comparison shows that precision of results varies between facilities: while DMaC displays improved precision for dynamic stiffness characterisation, other stiffness measures are more precise at IFREMER. It is difficult to attribute this variance to difference in the facilities or variation in sample quality without further investigations.

Both facilities provide the highest and lowest precision for quasi-static and break stiffness values, respectively. Moreover, the quasi-static stiffness displays the least variation between facilities and can be regarded as most representative of the actual stiffness. On the contrary, the dynamic stiffness values display the largest difference between the facilities, therefore, the results have a relatively lower accuracy.

It is found that the ISO protocol for offshore polyester moorings is suitable for MRE applications; however, it is recommended that the guidance should be extended to incorporate higher loading frequencies, in order to improve rope dynamic response assessment.

The tensile properties of the hybrid polyester-polyolefin ropes tested are intermediate between those of 100% polyester and 100% polyamide 6, and this material provides an additional option for high extension mooring ropes for MRE applications. Rope modelling suggests that further energy absorption may be possible in hybrid ropes by adjusting rope construction parameters.

Author Contributions: Conceptualisation, F.K. and P.D.; Data curation, P.H. and N.L.; Formal analysis, F.K. and P.D.; Funding acquisition, L.J.; Investigation, F.K., P.H., N.L. and P.D.; Supervision, L.J.; Validation, P.D.; Visualisation, F.K. and P.D.; Writing—original draft, F.K. and P.D.; Writing—review and editing, P.H., P.R.T., P.D. and L.J. All authors have read and agreed to the published version of the manuscript.

Funding: This research received funding from the European Union Horizon 2020 Framework Programme (H2020) under grant agreement no 731084 of the Marine Renewables Infrastructure Network for emerging Energy Technologies (MaRINET2) project.

Conflicts of Interest: The authors declare no conflict of interest.

References

1. DelVecchio, C.J.M. Light Weight Materials for Deep Water Moorings. Ph.D. Thesis, University of Reading, Reading, UK, 1992.
2. De Pellegrin, I. Manmade fiber ropes in deepwater mooring applications. In Proceedings of the Offshore Technology Conference, Houston, TX, USA, 3–6 May 1999.
3. Bugg, D.L.; Vickers, D.T.; Dorchak, C.J. Mad Dog project: Regulatory approval process for the new technology of synthetic (polyester) moorings in the Gulf of Mexico. In Proceedings of the Offshore Technology Conference, Houston, TX, USA, 3–6 May 2004.
4. Flory, J.; Berryman, C.; Banfield, S.J. Polyester mooring lines on platforms and MODUs in deep water. In Proceedings of the Offshore Technology Conference, Houston, TX, USA, 30 April–3 May 2007.
5. Davies, P.; Weller, S.D.; Johanning, L.; Banfield, S.J. A review of synthetic fiber moorings for marine energy applications. In Proceedings of the 5th International Conference on Ocean Energy 2014, Halifax, NS, Canada, 4–6 November 2014.
6. Weller, S.D.; Johanning, L.; Davies, P.; Banfield, S.J. Synthetic mooring ropes for marine renewable energy applications. *Renew. Energy* **2015**, *83*, 1268–1278.
7. Ridge, I.M.L.; Banfield, S.J.; Mackay, J. Nylon fibre rope moorings for wave energy converters. In Proceedings of the Oceans MTS/IEEE 2010, Seattle, WA, USA, 20–23 September 2010.
8. Pham, H.D.; Cartraud, P.; Schoefs, F.; Soulard, T.; Berhault, C. Dynamic modeling of nylon mooring lines for a floating wind turbine. *Appl. Ocean Res.* **2019**, *87*, 1–8.
9. Chevillotte, Y.; Marco, Y.; Bles, G.; Devos, K.; Keryer, M.; Arhant, M.; Davies, P. Fatigue of improved polyamide mooring ropes for floating wind turbines. *Ocean Eng.* **2020**, *199*, 107011.
10. McKenna, H.A.; Hearle, J.W.S.; O'Hear, N. *Handbook of Fibre Rope Technology*; Elsevier: Amsterdam, The Netherlands, 2004.
11. Francois, M.; Davies, P. Fibre rope deep water mooring: A practical model for the analysis of polyester mooring systems. In Proceedings of the Oil Gas Conference, Rio de Janeiro, Brazil, 16–19 October 2000.
12. Sloan, F.; Bull, S.; Longerich, R. Design modifications to increase fatigue life of fiber ropes. In Proceedings of the Oceans MTS/IEEE 2005, Seattle, WA, USA, 19–23 September, 2005.
13. Gordelier, T.; Parish, D.; Thies, P.; Johanning, L. A Novel Mooring Tether for Highly-Dynamic Offshore Applications; Mitigating Peak and Fatigue Loads via Selectable Axial Stiffness. *J. Mar. Sci. Eng.* **2015**, *3*, 1287–1310.
14. Davies, P.; Weller, S.; Johanning, L. *D3.5.1 MERiFIC—Testing of Synthetic Fibre Ropes*; IFREMER: Brest, France, 2012.
15. Moylan, S.; Brown, C.U.; Slotwinski, J. Recommended Protocol for Round-Robin Studies in Additive Manufacturing. *J. Test. Eval.* **2016**, *44*, 1009–1018.
16. Pitkethly, M.J.; Favre, J.P.; Gaur, U.; Jakubowski, J.; Mudrich, S.F.; Caldwell, D.L.; Drzal, L.T.; Nardin, M.; Wagner, H.D.; Di Landro, L.; et al. A round-robin programme on interfacial test methods. *Compos. Sci. Technol.* **1993**, *48*, 205–214.
17. Venosa, A.D.; King, D.W.; Sorial, G.A. The baffled flask test for dispersant effectiveness: A round robin evaluation of reproducibility and repeatability. *Spill Sci. Technol. Bull.* **2002**, *7*, 299–308.
18. Sheng, S. *Wind Turbine Gearbox Condition Monitoring Round Robin Study-Vibration Analysis*; NREL: Golden, CO, USA, 2012.
19. ISO. *Fibre Ropes for Offshore Station Keeping*; Polyester ISO 18692; ISO publications: Geneva, Switzerland, 2007.
20. ISO. *Fibre Ropes for Offshore Station Keeping*; Polyarylate ISO/TS 19336; ISO publications: Geneva, Switzerland, 2015.
21. Banfield, S.J.; Flory, J.F. Computer modelling of large, high-performance fiber rope properties. In Proceedings of the Oceans'95 MTS/IEEE, San Diego, CA, USA, 9–12 October 1995; Volume 3, pp. 1563–1571.
22. Hearle, J.W.S.; Parsey, M.R.; Overington, M.S.; Banfield, S.J. Modelling the long-term fatigue performance of fibre ropes. In Proceedings of the Third International Offshore and Polar Engineering Conference, Singapore, 6–11 June 1993.

23. Leech, C.M.; Hearle, J.W.S.; Overington, M.S.; Banfield, S.J. Modelling tension and torque properties of fibre ropes and splices. In Proceedings of the Third International Offshore and Polar Engineering Conference Singapore, 6–11 June 1993.
24. Flory, J.F.; Leech, C.M.; Banfield, S.J.; Petruska, D.J. Computer model to predict long-term performance of fiber rope mooring lines. In Proceedings of the Offshore Technology Conference, Houston, TX, USA, 2–5 May 2005.
25. Davies, P.; Bouquet, P.; Conte, M.; Deuff, A. Tension/torsion behavior of deepwater synthetic mooring lines. In Proceedings of the Offshore Technology Conference, Houston, TX, USA, 1–4 May 2006.
26. Lechat, C.; Bunsell, A.R.; Davies, P. Tensile and creep behaviour of polyethylene terephthalate and polyethylene naphthalate fibres. *J. Mater. Sci.* **2010**, *46*, 528–533.
27. Vaseghi, R. A New Method of Termination for Heavy-Duty Synthetic Rope Fibres. Ph.D. Thesis, Bournemouth University, Bournemouth, UK, 2004.
28. Leech, C.M. The modelling and analysis of splices used in synthetic ropes. *Proc. R. Soc. A Math. Phys. Eng. Sci*. **2003**, *459*, 1641–1659.
29. Banfield, S.J.; Flory, J.F.; Hearle, J.W.; Overington, M.S. Comparison of fatigue data for polyester and wire ropes relevant to deepwater moorings. In Proceedings of the 18th International Conference on Offshore Mechanics and Arctic Engineering Proceedings, St. John's, NF, Canada, 11–16 July 1999.

© 2020 by the authors. Licensee MDPI, Basel, Switzerland. This article is an open access article distributed under the terms and conditions of the Creative Commons Attribution (CC BY) license (http://creativecommons.org/licenses/by/4.0/).